International Journal of Robotics and Control Systems
Vol. 4, No. 2, 2024, pp. 814-831
ISSN 2775-2658
http://pubs2.ascee.org/index.php/ijrcs

# Cascade PID Control for Altitude and Angular Position Stabilization of 6-DOF UAV Quadcopter

Trinh Luong Mien [a,1,*], Tran Ngoc Tu [a,2], Vo Van An [b,3]

[a] University of Transport and Communications, Hanoi, Vietnam
[b] Eastern International University, Binh Duong, Vietnam
[1] mientl@utc.edu.vn; [2] tutn@utc.edu.vn; [3] an.vovan@eiu.edu.vn
* Corresponding Author

ARTICLE INFO

**Article history**
Received April 10, 2024
Revised May 12, 2024
Accepted May 29, 2024

**Keywords**
UAV Control;
Flight Stability;
Cascade Control;
Ziegler-Nichols;
PID Tuning;
Modeling;
Matlab

ABSTRACT

UAVs are commonly used in transportation, especially in the express delivery of light cargo parcels. However, controlling UAVs is difficult because of their complex structure and wide range of operations in space. The research contribution is proposed a cascade control structure using six PID controllers for the 6-DOF UAV quadcopter, that ensures the altitude angulars positions control at the desired values and maintains flight balance stability for the 6-DOF UAV quadcopter. First, the mathematical dynamic models for the 6-DOF UAV quadcopter have been researched and developed, including the translational dynamic mathematical model and the rotational dynamic mathematical model of the 6-DOF UAV quadcopter. This is a complex object with strong nonlinearity and difficult control. And then, the article introduces the method of designing six PID controllers for 6-DOF UAV quadcopter to meet the requirements, based on applying the Ziegler-Nichols experimental method. Applying the Ziegler-Nichols experimental method makes the process of designing a UAV quadcopter control system simple, straightforward and heuristics with fast controller parameters tuning. Next, the article presents the results of modeling and simulation of the 6-DOF UAV quadcopter control system on Matlab/Simulink. The simulation results show that the six proposed PID controllers have ensured the flight balance stability at the desired altitude and angular positions with overshoot less than 20%, steady-state error less than 1%. This shows the prospect of applying the proposed PID control method to physical UAVs, easily adjusting PID parameters to suit the flight environment.



## 1. Introduction

In recent years, unmanned aerial vehicles (UAVs) have shown significant market potential to significantly reduce costs and time in the logistics sector. The use of UAVs to provide commercial courier services has become an emerging industry, dramatically changing the delivery of the freight industry. In particular, the use of small quadcopter UAVs to transport and distribute envelopes and small, lightweight parcels of goods is becoming increasingly popular.

The UAV quadcopter have four propellers attached to the body by the arm. The propellers are driven by electric motors, which allow the drone to fly up, down, forward, backwards, left, right and

rotate. The quadcopter UAVs are versatile and can be used for various purposes, such as photography and videography, delivery, pesticide spraying, agricultural granulation, search and rescue, military service, security and defence, and other applications.

However, precisely because of the quadcopter UAVs flexibility and efficiency in transporting goods, in performing other tasks, their mechanical structure and control system are complex. UAV quadcopter is a strong nonlinear control object and difficult flight control in space. Common quadcopter UAV control tasks are flight stability control, flight position control, orbital control and research focuses on this task.

Scientific research works on UAVs often start from their basic dynamics model, incorporating more complex aerodynamic features [1], [2]. The proposed UAV control methods include backstepping control [3], [4], fuzzy logic control [5], [6], proportional-integral-derivative (PID) control [7], [8], [13], [15], [17]-[20], [24]-[27], [30], [31], [34], [35], [41]-[43], [45]-[48], linear quadratic regulator [9], model predictive control [10], feedback linearization control [11], sliding mode control (SMC) [12], [38], [39], optimal control [14], [21], optimized PID control [16], [33], nonlinear robust control [22], advanced PID control [23], neuron network based PID control [29], [40], nonlinear control [32], adaptive PID control [44], PID control and integral state feedback [49], extended Kalman filter and adaptive fuzzy PID control [50], fuzzy-PID control [51], [52]. These studies share the common goal of studying the UAV mathematical model and developing appropriate algorithms to stabilize and control the movement trajectory of UAVs. The research works to develop UAV control solutions based on PID or PID combined with other methods, such as fuzzy logic, neural networks, optimization algorithms, swarm optimization, genetic algorithms, has brought initial results on UAV flight stability control and UAV trajectory tracking control. However, the published studies provide control algorithms that are difficult to implement, hide important controller information, and do not provide specific UAV controller design procedures, especially the controller parameter adjustment procedures to suit various types of UAVs or consider external disturbance on the UAV.

The main content of this article focuses on the dynamic model of UAV quadcopter and designs the 6-DOF UAV quadcopter PID cascade control system ensuring altitude angulars positions control. The 6-DOF UAV quadcopter PID controllers are synthesized based on the Ziegler-Nichols experimental method. The research contribution in this article is the proposal of the cascade control structure using six PID controllers for the 6-DOF UAV quadcopter, ensuring altitude angulars positions control at the desired values and maintaining flight balance stability for the 6-DOF UAV quadcopter, and proceed to synthesize UAV quadcopter Euler angle PID controllers and UAV quadcopter x, y, z position PID controllers. This proposed control structure is implemented simply, without complexity and with quick parameters heuristic adjustment.

The structure of this article consists of five main parts. Part 1 presents an overview of UAV quadcopter control. Part 2 presents the mathematical dynamic models of the 6-DOF UAV quadcopter, included the translational dynamic model and the rotational dynamic model. Part 3 proposes a cascade control structure using six PID controllers for the 6-DOF UAV quadcopter and design six PID controllers for 6-DOF UAV quadcopter, based on applying the Ziegler-Nichols experimental method. Part 4 presents the results of modeling and simulation of the 6-DOF UAV quadcopter control system on Matlab/Simulink. Final part provides conclusions about the advantages and disadvantages of the proposed method and future research.

## 2. Dynamic Models of 6-DOF UAV Quadcopter

The structural diagram of the UAV quadcopter is shown in Fig. 1, including the angular velocity, torque, and the corresponding force generated by the four rotors, which include the four propellers, driven by four electrical motors, numbered from 1 to 4.

The UAV's absolute translational position in the inertial frame x, y, z-axes, attached to the ground, is denoted $\boldsymbol{\xi}$, $\xi=[x\ y\ z]^T$. The angular position is determined by the Euler angles, $\eta$, $\eta=[\phi\ \theta\ \psi]^T$. The roll angle $\phi$determines the rotation of the UAV quadcopter around the x-axis. The

pitch angle $\theta$ determines the rotation of the UAV quadcopter around the y-axis. The yaw angle $\psi$ determines the rotation of the UAV quadcopter the z-axis. The vector $\boldsymbol{\varepsilon}$ is combination of the translational position vetor $\boldsymbol{\xi}$ and the angular position vetor $\boldsymbol{\eta}$,ε=[ξ η].

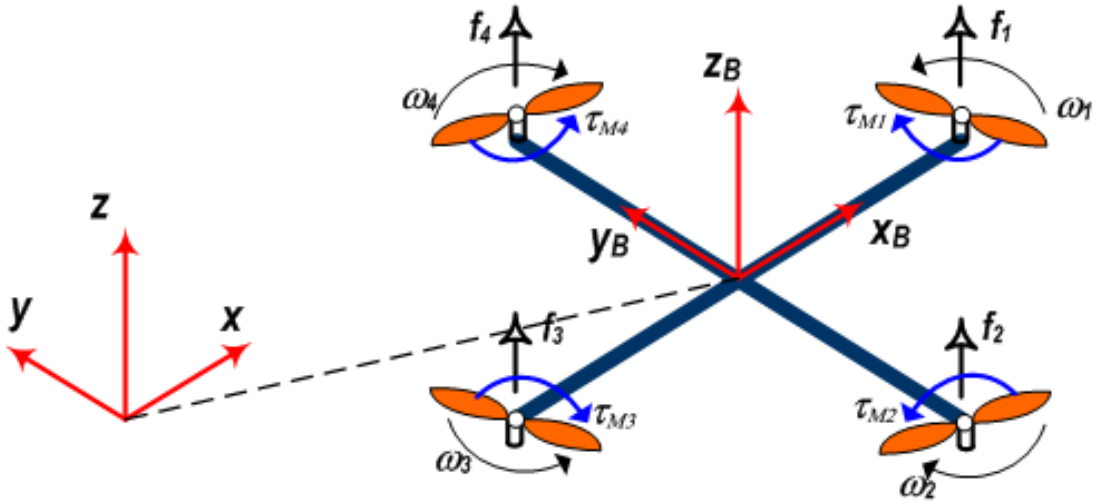


**Fig. 1.** Inertial reference frame and body reference frame of quadcopter UAVs

The UAV's body frame has the origin point that is the UAV's center of mass point. In the UAV's body frame, translational velocities are denoted by $V_B$ and angular velocities by$\boldsymbol{\nu}$.

$$V_B = [v_{x,B}\ v_{y,B}\ v_{z,B}]^T, \nu = [p\ q\ r]^T \tag{1}$$

The rotation matrix from the body frame to the inertial frame is determined *R*, [13]-[16], [36], [37].

$$\mathrm{R}=\begin{bmatrix} C_\psi C_\theta & C_\psi S_\theta S_\phi - S_\psi C_\theta & C_\psi S_\theta C_\phi + S_\psi S_\phi \\ S_\psi C_\theta & S_\psi S_\theta S_\phi + C_\psi C_\theta & S_\psi S_\theta C_\phi - C_\psi S_\phi \\ -S_\theta & C_\theta S_\phi & C_\theta C_\phi \end{bmatrix} \tag{2}$$

Where $S_\psi = sin(\psi), C_\psi = cos(\psi)$. The rotation matrix *R* is orthogonal, so that$R^{-1}$=R$^T$which is the rotation matrix from the inertial frame to the body frame.

The matrix that transforms the angular velocity from the inertial frame to the body frame is $W_\eta$ and from the body frame to the inertial frame is $W_\eta^{-1}$ [13], [17].

$$\mathrm{v}=\mathrm{W}_\eta\dot{\eta} \quad \begin{bmatrix} p \\ q \\ r \end{bmatrix} = \begin{bmatrix} 1 & 0 & -S_\theta \\ 0 & C_\phi & C_\theta S_\phi \\ 0 & -S_\phi & C_\theta C_\phi \end{bmatrix} \begin{bmatrix} \dot{\phi} \\ \dot{\theta} \\ \dot{\psi} \end{bmatrix}$$

$$\dot{\eta}=\mathrm{W}_\eta^{-1}\mathrm{v} \quad \begin{bmatrix} \dot{\phi} \\ \dot{\theta} \\ \dot{\psi} \end{bmatrix} = \begin{bmatrix} 1 & S_\phi T_\theta & C_\phi T_\theta \\ 0 & C_\phi & -S_\phi \\ 0 & S_\phi/C_\theta & S_\phi/C_\theta \end{bmatrix} \begin{bmatrix} p \\ q \\ r \end{bmatrix} \tag{3}$$

Where, $T_\phi = tan(\phi)$; $W_\eta$ is reversible in the case of $\theta \neq (2k-1)\frac{\phi}{2}, k = 1,2,$

Assuming that the UAV quadcopter has a symmetrical structure with four arms aligned with the body x-axis and y-axis. Thus, the inertia matrix is diagonal matrix *I*, is defined as.

$$\mathrm{I}=\begin{bmatrix} I_{xx} & 0 & 0 \\ 0 & I_{yy} & 0 \\ 0 & 0 & I_{zz} \end{bmatrix} \tag{4}$$

The angular velocity of the *i*-rotor, denoted by$\omega_i$, generated the lift fore $f_i$ in the direction of the rotor axis. In addition, the angular velocity and acceleration also generate the torque $\tau_{Mi}$, around the rotor shaft [13], [18].

$$f_i = k\omega_i^2, \tau_{M_i} = b\omega_i^2 + I_M\dot{\omega}_i \simeq b\omega_i^2 \tag{5}$$

Where, $k$ is the lift force coefficient, $b$ is the torque coefficient of the rotor, and $I_M$ is the moment of inertia of the rotor. Since the propeller is so light, the $\dot{\omega}_i$effect is often omitted.

The combination of the four lift rotors foces create the $F$ thrust force in direction of the body along z-axis. Total torque$\tau_B$ consists of torques $\tau_\phi, \tau_\theta$and $\tau_\psi$in the direction of the corresponding body frame angles [13], [19].

$$F = \sum_{i=1}^{4} f_i = k\sum_{i=1}^{4}\omega_i^2, F_B = \begin{bmatrix}0\\0\\F\end{bmatrix} \tag{6}$$

$$\tau_B = \begin{bmatrix}\tau_\phi\\\tau_\theta\\\tau_\psi\end{bmatrix} = \begin{bmatrix}l\,k\,(\omega_4^2 - \omega_2^2)\\l\,k\,(\omega_3^2 - \omega_1^2)\\b(\omega_1^2 - \omega_2^2 + \omega_3^2 - \omega_4^2)\end{bmatrix} \tag{7}$$

where $l$ is the distance from the UAV's centre to the propeller.

The roll $\phi$ angle adjustment is achieved by increasing the 4th rotor angular velocity and decreasing the 2nd rotor angular velocity. The pitch $\theta$ angle adjustment is achieved by increasing the 3rd rotor angular velocity and decreasing the 1st rotor angular velocity. The yaw $\Psi$ angle adjustment is achieved by increasing the angular velocities of two opposite 1,3 rotors and decreasing the angular velocities of two other 2,4 rotors.

### 2.1. Dynamic Model of UAV Quadcopter Using Newton-Euler Equations

Considering a quadcopter UAV as a rigid object, we can analyze its dynamics using Newton-Euler equations. In the body frame, the force required to generate mass acceleration $m\dot{V}_B$ and centrifugal force $\nu \times (mV_B)$ equal to gravity $R^T G$ and the thrust force of the rotors $F_B$, [13], [20].

$$m\dot{V}_B + \nu \times (mV_B) = R^T G + F_B \tag{8}$$

In the inertial frame, the centrifugal force is zero and, therefore, the translational acceleration of a quadcopter UAV is affected only by the force of gravity, magnitude and direction of the thrust forces [20].

$$m\ddot{\xi} = G + \mathrm{R}F_B$$

$$\begin{bmatrix}\ddot{x}\\\ddot{y}\\\ddot{z}\end{bmatrix} = -g\begin{bmatrix}0\\0\\1\end{bmatrix} + \frac{F}{m}\begin{bmatrix}C_\psi S_\theta C_\phi + S_\psi S_\phi\\S_\psi S_\theta C_\phi - C_\psi S_\phi\\C_\theta C_\phi\end{bmatrix} \tag{9}$$

In the body frame, the angular acceleration of inertia Iν̇, centripetal forces$\nu \times (\mathrm{I}\nu)$ and gyros forces $\delta$ are equal to the by external torque $\tau_B$.

$$\mathrm{I}\dot{\nu} + \nu \times (\mathrm{I}\nu) + \delta = \tau_B$$

$$\dot{\nu} = I^{-1}\left(-\begin{bmatrix}p\\q\\r\end{bmatrix} \times \begin{bmatrix}I_{xx}p\\I_{yy}q\\I_{xx}r\end{bmatrix} - I_M\begin{bmatrix}p\\q\\r\end{bmatrix} \times \begin{bmatrix}0\\0\\1\end{bmatrix}\omega_\delta + \tau_B\right)$$

$$\begin{bmatrix}\dot{p}\\\dot{q}\\\dot{r}\end{bmatrix} = \begin{bmatrix}(I_{yy} - I_{zz})qr/I_{xx}\\(I_{zz} - I_{xx})pr/I_{yy}\\(I_{xx} - I_{yy})pq/I_{zz}\end{bmatrix} - I_M\begin{bmatrix}q/I_{xx}\\-p/I_{yy}\\0\end{bmatrix}\omega_\delta + \begin{bmatrix}\tau_\phi/I_{xx}\\\tau_\theta/I_{yy}\\\tau_\Psi/I_{zz}\end{bmatrix} \tag{10}$$

where, $\omega_\delta = \omega_1 - \omega_2 + \omega_3 - \omega_4$.

The angular accelerations in the inertial frame are the time derivative of the angular velocities in the body frame, converted using the transformation matrix $W_\eta^{-1}$.

$$\ddot{\eta} = \frac{d}{dt}(W_\eta^{-1}\nu) = \frac{d}{dt}(W_\eta^{-1})\nu + W_\eta^{-1}\dot{\nu}$$

$$\ddot{\eta} = \begin{bmatrix} 0 & \dot{\phi}C_\phi T_\theta + \dot{\theta}S_\phi / C_\theta^2 & -\dot{\phi}S_\phi C_\theta + \dot{\theta}C_\phi / C_\theta^2 \\ 0 & -\dot{\phi}S_\phi & -\dot{\phi}C_\phi \\ 0 & \dot{\phi}C_\phi / C_\theta + \dot{\phi}S_\phi T_\theta / C_\theta & -\dot{\phi}S_\phi / C_\theta + \dot{\theta}C_\phi T_\theta / C_\theta \end{bmatrix} \nu + W_\eta^{-1}\dot{\nu} \quad (11)$$

## 2.2. Dynamic Model of UAV Quadcopter Using Euler–Lagrange Equations

Lagrange function $\boldsymbol{L}$ is the sum of rotational energy $E_{rot}$ and translational energy $E_{trans}$ minus potential energy $E_{pot}$ [13], [20].

$$L = E_{trans} + E_{rot} - E_{pot} = \frac{m}{2}\dot{\xi}^T\dot{\xi} + \frac{1}{2}\nu^T \mathrm{I}\nu - mgz \quad (12)$$

Euler - Lagrange equations with external forces and torques are as [13], [20], [21].

$$\begin{bmatrix} f \\ \tau \end{bmatrix} = \frac{d}{dt}\left(\frac{\partial L}{\partial \dot{\varepsilon}}\right) - \frac{\partial L}{\partial \varepsilon} \quad (13)$$

Where, $\tau$denotes the rotational torques, and$f$ is the translational forces. The translational and rotational components are independent [13], [22], so they can be studied separately. The translational Euler–Lagrange equations are as below, which is equivalent with equations (9).

$$f = \mathrm{RF}_B = m\ddot{\xi} + mg\begin{bmatrix} 0 \\ 0 \\ 1 \end{bmatrix} \quad (14)$$

The overall dynamics of UAV quadcopter are divided into translational and rotational motion by considering the corresponding state vectors. Translational motion can be represented by a fixed angle as follows [22].

$$\begin{aligned} m\ddot{x} + A_x\dot{x} &= F(\cos\psi \sin\theta \cos\phi + \sin\psi \sin\phi) \\ m\ddot{y} + A_y\dot{y} &= F(\sin\psi \sin\theta \cos\phi - \cos\psi \sin\phi) \\ m\ddot{z} + mg + A_z\dot{z} &= F(\cos\phi \cos\theta) \end{aligned} \quad (15)$$

Where $F$ is the thrust force acting along the z-axis. $A_x, A_y, A_z$ are the coefficients of air resistance in the corresponding directions of the axes of the inertial frame.

Applying the Euler angles of the object to the equation (15), it can be seen that the acceleration ignoring air resistance would as below [23].

$$\begin{aligned} m\ddot{x} &= F(\cos\psi \sin\theta \cos\phi + \sin\psi \sin\phi) \\ m\ddot{y} &= F(\sin\psi \sin\theta \cos\phi - \cos\psi \sin\phi) \\ m\ddot{z} &= F(\cos\phi \cos\theta) - mg \end{aligned} \quad (16)$$

Therefore, the translational motion equations of UAV quadcopter as.

$$\ddot{x} = \frac{F}{m}(\cos\psi \sin\theta \cos\phi + \sin\psi \sin\phi) \quad (17)$$

$$\ddot{y} = \frac{F}{m}(sin\,\psi\,sin\,\theta\,cos\,\phi - cos\,\psi\,sin\,\phi)$$

$$\ddot{z} = \frac{F}{m}(cos\,\phi\,cos\,\theta) - g$$

In addition, the Jacobian matrix $J(\eta)$ from $\nu$ to $\dot{\eta}$ is defined as follows [13], [21], [22].

$$J(\eta) = J = W_\eta^T \mathrm{I}\, W_\eta$$
$$J = \begin{bmatrix} I_{xx} & 0 & -I_{xx}S_\theta \\ 0 & I_{yy}C_\phi^2 + I_{zz}S_\phi^2 & (I_{yy} - I_{zz})C_\phi S_\phi C_\theta \\ -I_{xx}S_\theta & (I_{yy} - I_{zz})C_\phi S_\phi C_\theta & I_{xx}S_\theta^2 + I_{yy}S_\phi^2 C_\theta^2 + I_{zz}C_\phi^2 C_\theta^2 \end{bmatrix} \quad (18)$$

The rotational energy can be represented in the inertial frame as below [13], [21], [22].

$$E_{rot} = \frac{1}{2}\nu^T \mathrm{I}\, \nu = \frac{1}{2}\ddot{\eta}^T \mathrm{J}\, \ddot{\eta} \quad (19)$$

The Euler-Lagrange equations with the external angular force – torques of the rotors, are.

$$\tau = \tau_B = \mathrm{J}\,\ddot{\eta} + \frac{d}{dt}(J)\,\dot{\eta} - \frac{1}{2}\frac{\partial}{\partial \eta}(\dot{\eta}^T \mathrm{J}\,\dot{\eta}) = \mathrm{J}\,\ddot{\eta} + C(\eta,\dot{\eta})\,\dot{\eta} \quad (20)$$

Where, the matrix $C(\eta,\dot{\eta})$ is Coriolis term, containing the gyros and centripetal terms.

The $C(\eta,\dot{\eta})$ matrix are as follows [13], [22].

$$C(\eta,\dot{\eta}) = \begin{bmatrix} C_{11} & C_{12} & C_{13} \\ C_{21} & C_{22} & C_{23} \\ C_{31} & C_{32} & C_{33} \end{bmatrix}$$

$$C_{11} = 0; C_{12} = \left(I_{yy} - I_{zz}\right)\left(\dot{\theta}C_\phi S_\phi + \dot{\psi}S_\phi^2 C_\theta\right) + \left(I_{zz} - I_{yy}\right)\dot{\psi}C_\phi^2 C_\theta - I_{xx}\dot{\psi}C_\theta; C_{13} = \left(I_{zz} - I_{yy}\right)\dot{\psi}C_\phi S_\phi C_\theta^2$$
$$C_{21} = \left(I_{zz} - I_{yy}\right)\left(\dot{\theta}C_\phi S_\phi + \dot{\psi}S_\phi C_\theta\right) + \left(I_{yy} - I_{zz}\right)\dot{\psi}C_\phi^2 C_\theta + I_{xx}\dot{\psi}C_\theta$$
$$C_{22} = \left(I_{zz} - I_{yy}\right)\dot{\phi}C_\phi S_\phi; C_{23} = -I_{xx}\dot{\psi}S_\theta C_\theta + I_{yy}\dot{\psi}S_\phi^2 S_\theta C_\theta + I_{zz}\dot{\psi}C_\phi^2 S_\theta C_\theta$$
$$C_{31} = \left(I_{yy} - I_{zz}\right)\dot{\psi}C_\theta^2 S_\phi C_\phi - I_{xx}\dot{\theta}C_\theta$$
$$C_{32} = \left(I_{zz} - I_{yy}\right)\left(\dot{\theta}C_\phi S_\phi S_\theta + \dot{\phi}S_\phi^2 C_\theta\right) + \left(I_{yy} - I_{zz}\right)\dot{\phi}C_\phi^2 C_\theta + I_{xx}\dot{\psi}S_\theta C_\theta - I_{yy}\dot{\psi}S_\phi^2 S_\theta C_\theta - I_{zz}\dot{\psi}C_\phi^2 S_\theta C_\theta$$
$$C_{33} = \left(I_{yy} - I_{zz}\right)\dot{\phi}C_\phi S_\phi C_\theta^2 - I_{yy}\dot{\theta}S_\phi^2 C_\theta S_\theta - I_{zz}\dot{\theta}C_\phi^2 C_\theta S_\theta + I_{xx}\dot{\theta}C_\theta S_\theta$$

From equation (20) leads to the differential equations for the angular accelerations which are equivalent with equations (10), (11), has the form, as shown in (21).

$$\ddot{\eta} = J^{-1}[\tau_B - C(\eta,\dot{\eta})\,\dot{\eta}] \quad (21)$$

## 3. Design of PID Controller for 6-DOF UAV Quadcopter

### 3.1. Method of the PID Parameters Adjustment for 6-DOF UAV Quadcopter

With the simple structure and easy implementation, the PID controller is deployed to stabilize the attitude and angles positions of 6-DOF UAV quadcopter. The general control law of the PID controller is mentioned in [13], [24]-[26], [40]. The general PID controller structure is shown in Fig. 2 [27]. Where, $e(t)$ is the difference between the desired state $x_d(t)$ and current state $x(t)$; $u(t)$ is the input signal that controls the process. The parameters for the proportional, integral, and derivative components of the PID controller are represented by $k_P, k_I, k_D$.

There are many methods for determining PID controller parameters for the process, among which the Tyreus-Luyben method [28], [29] and the Ziegler-Nichols method [28], [30] allow experimentation on the system model, using the proportional component P and adjustment $k_P$ until the system response achieves the cyclic oscillation. The critical frequency values, $t_{th}$ and the critical amplification value, $k_{th}$, is used to determine the PID controller's parameters. This is one of the most conservative approaches to fine-tuning controller parameters to improve the UAV control quality.

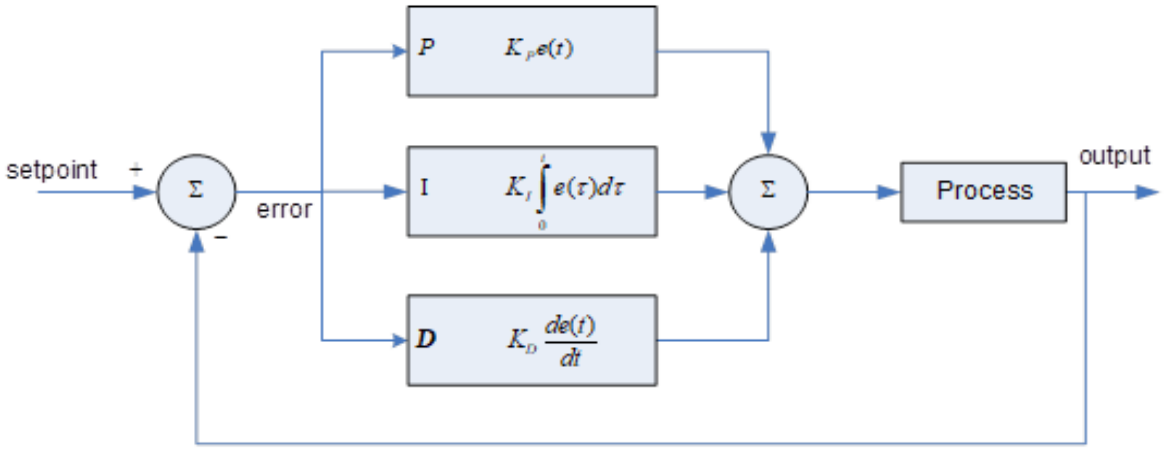


**Fig. 2.** The general structure of PID controller

$$e(t) = x_d(t) - x(t)$$
$$u(t) = k_P e(t) + k_I \int_0^t e(\tau)d\tau + k_D \frac{de(t)}{dt} \quad (22)$$

Fig. 3 presents the typical diagram for determining the PID controller parameters for the yaw $\psi$ angle control loop of UAV quadcopter, using the Ziegler-Nichols method.

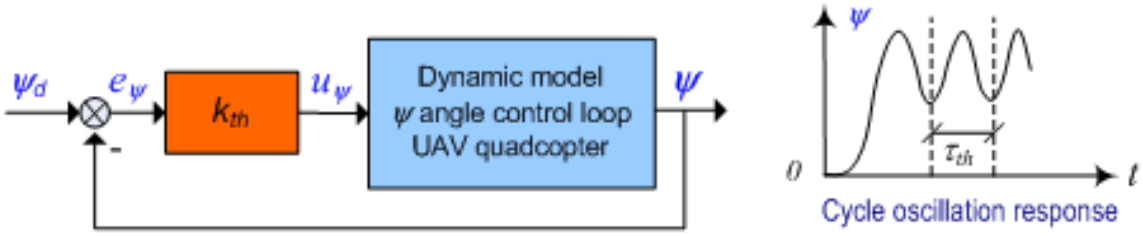


**Fig. 3.** The PID controller parameters, determined based on the Ziegler-Nichols method

According to the Ziegler-Nichols method [28], [30], the PID controller parameters for the yaw $\psi$ angle control loop of UAV quadcopter is defined by formulas below.

$$k_{P\psi} = 0.6k_{th\psi}; k_{I\psi} = \frac{2k_{P\psi}}{\tau_{th\psi}}; k_{D\phi} = \frac{k_{P\psi}\tau_{th\psi}}{8} \quad (23)$$

The PID controller parameters are selected based on the characteristics of each component proportional P, integral I and differential D, as shown in Table 1.

**Table 1.** The PID control law characteristics

| Parameter | Rise time | Steady time | Overshot | Steady error |
|---|---|---|---|---|
| $k_P$ | Decrease | Increase | Small change | Decrease |
| $k_I$ | Decrease | Increase | Increase | Eliminate |
| $k_D$ | Small change | Decrease | Decrease | Small change |

Based on Table 1, we test the P component, by adjusting $k_P$ so that the response time is fast enough, accepting a small overshoot adjustment. Then, add component D to remove overshoot, by increasing $k_D$, experiment gradually and select the appropriate value. Stability steady-errors may appear. Finally, component I is also added to reduce the stability steady-error, $k_I$ should be increased from small to large to reduce the stability steady-error and, simultaneously, not let the over-correction reappear.

### 3.2. Proposed the PID Cascade Structure for 6-DOF UAV Quadcopter

The UAV quadcopter has four control inputs, four rotor angular velocity, $\omega_i$ but there are six states, position $\boldsymbol{\xi}$ and angular $\boldsymbol{\eta}$. Equations (9), (10), (11) determine the dynamics of the UAV quadcopter, denoting the interaction between states and the total thrust force $\boldsymbol{f}$ and torque$\boldsymbol{\tau}$ generated by the rotors. The UAV quadcopter is kept the attitude position thanks to total thrust force $\boldsymbol{f}$, which also affects acceleration along the z-axis. Acceleration of the angle $\phi$ affected by torque $\tau_\phi$, acceleration of the angle $\theta$ affected by torque $\tau_\theta$, and acceleration of the angle $\psi$ is powered by torque $\tau_\psi$ [13], [31]-[33]. The PID controllers' structure block diagram for the 6-DOF UAV quadcopter is shown in Fig. 4.

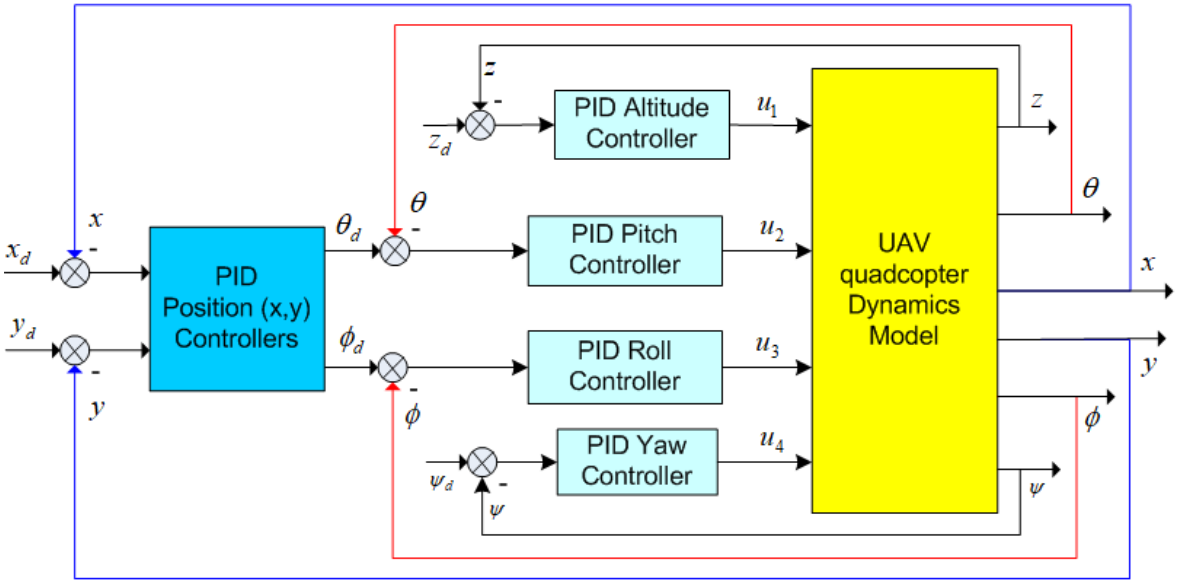


**Fig. 4.** The PID controllers' cascade structure block diagram for 6-DOF UAV quadcopter

The PID controllers' structure for UAV quadcopter include the two single-feedback control loops: attitude loop z and yaw angle loop $\Psi$; and two cascade-feedback control loops: roll and pitch angle feedback control loops – inner control loops, and outer control loops – x, y positon feedback control loops.

The method of determining the parameters of PID controllers for UAV quadcopter, according to the Ziegler-Nichols experimental method, based on observing the closed-loop cycle oscillation response with each control loop at $k_{th}$ and $t_{th}$ values, is summarized as follows:

- Step 1. Conducting yaw angle $\psi$ control loop experiment, as shown in Fig. 3, by adjusting $k_P$ to the$k_{th}$value corresponding to the cycle oscillation output response, and then determine the oscillation cycle period $t_{th}$
- Step 2. Based on $k_{th}$and $t_{th}$, calculate the PID parameters according (23) for the yaw angle $\psi$ control loop:$k_{P\psi}$,$k_{I\psi}$, $k_{D\psi}$
- Step 3. Conducting the similar experiments with the other control loops: *z*-altitude control loop, $\phi$-angle control loop, $\theta$-angle control loop and *x*,*y*-position control loops.

### 3.3. Design of the PID Angles and Attitude Controllers for 6-DOF UAV Quadcopter

The PID controllers calculate the total thrust force and rotor torques for the UAV quadcopter, which are defined by formulas as shown in (24).

$$\begin{aligned} F &= (g + K_{Pz}(z_d - z) + K_{Iz}\int (z_d - z) + K_{Dz}(\dot{z}_d - \dot{z}))\frac{m}{C_\phi C_\theta} \\ \tau_\phi &= (K_{P\phi}(\phi_d - \phi) + K_{I\phi}\int (\phi_d - \phi) + K_{D\phi}(\dot{\phi}_d - \dot{\phi}))I_{xx} \\ \tau_\theta &= (K_{P\theta}(\theta_d - \theta) + K_{I\theta}\int (\theta_d - \theta) + K_{D\theta}(\dot{\theta}_d - \theta))I_{yy} \\ \tau_\psi &= (K_{P\psi}(\psi_d - \psi) + K_{I\psi}\int (\psi_d - \psi) + K_{D\psi}(\dot{\psi}_d - \dot{\psi}))I_{zz} \end{aligned} \quad (24)$$

Where, $g$ is the gravity, $m$ is the mass and $I_{xx}$, $I_{yy}$, $I_{zz}$ is inertia moment of the UAV quadcopter

According to the Ziegler-Nichols method [28], [30], the PID controllers parameters control the UAV quadcopter according to the angles $(\phi, \theta, \psi)$ control loops, and the altitude ($z$) control loop of the UAV quadcopter are determined by formulas as shown in (25).

$$\begin{aligned} k_{P\phi} &= 0.6k_{th\phi}; k_{I\phi} = \frac{2k_{P\phi}}{\tau_{th\phi}}; k_{D\phi} = \frac{k_{P\phi}\tau_{th\phi}}{8} \\ k_{P\theta} &= 0.6k_{th\theta}; k_{I\theta} = \frac{2k_{P\theta}}{\tau_{th\theta}}; k_{D\theta} = \frac{k_{P\theta}\tau_{th\theta}}{8} \\ k_{P\psi} &= 0.6k_{th\psi}; k_{I\psi} = \frac{2k_{P\psi}}{\tau_{th\psi}}; k_{D\phi} = \frac{k_{P\psi}\tau_{th\psi}}{8} \\ k_{Pz} &= 0.6k_{thz}; k_{Iz} = \frac{2k_{Pz}}{\tau_{thz}}; k_{Dz} = \frac{k_{Pz}\tau_{thz}}{8} \end{aligned} \quad (25)$$

### 3.4. Design of the PID Position Controllers for 6-DOF UAV Quadcopter

Arcoding to the above-mentioned control structure, the four inner feedback control loops are three angles and altitude. Two outer feedback loops are performed to adjust the x and y positions of the UAVquadcopter. The desired roll and pitch angles are the output of the outer control loops, and they serve as the input of the inner control loops, respectively, the desired angle, $\phi_d$, $\theta_d$, (Fig. 4)

When the UAV quadcopter is stable in the space, the roll angle $\phi$ and pitch angle $\theta$ have small values. Therefore, by using small angle assumptions, $S_{\phi_d} \equiv \phi_d, S_{\theta_d} \equiv \theta_d, C_{\phi_d} = C_{\theta_d} = 1$, the kinematic equations for the $x, y$ coordinates are simplified in equation as belows [34], [35].

$$\begin{aligned} \ddot{x} &= \frac{u_1}{m}(\theta_d \cos\psi + \phi_d \sin\psi) \\ \ddot{y} &= \frac{u_1}{m}(\theta_d \sin\psi\, s - \phi_d \cos\psi) \end{aligned} \quad (26)$$

With $u_1$ is the UAV quadcopter altitude control input signal

The altitude control PID controller is selected as follows:

$$u_1 = K_{Pz}(z_d - z) + K_{Iz}\int (z_d - z) + K_{Dz}(\dot{z}_d - \dot{z}) \quad (27)$$

Equation (26) is written as a matrix as follows.

$$\begin{bmatrix} \ddot{x} \\ \ddot{y} \end{bmatrix} = \frac{u_1}{m}\begin{bmatrix} S_\psi & C_\psi \\ -C_\psi & S_\psi \end{bmatrix}\begin{bmatrix} \phi_d \\ \theta_d \end{bmatrix} \quad (28)$$

Therefore, the desired pitch and roll control angles are determined by the formulas.

$$\begin{aligned}\phi_d &= (u_x \sin\psi - u_y \cos\psi)\\ \theta_d &= (u_x \cos\psi + u_y \sin\psi)\end{aligned} \tag{29}$$

Where, $u_x$ and $u_y$ are input control signals using the PID controller.

$$\begin{aligned}u_x &= K_{Px}(x_d - x) + K_{Ix}\int(x_d - x) + K_{Dx}(\dot{x}_d - \dot{x})\\ u_y &= K_{Py}(y_d - y) + K_{Iy}\int(y_d - y) + K_{Dy}(\dot{y}_d - \dot{y})\end{aligned} \tag{30}$$

According to the Ziegler-Nichols method [28], [30], the PID controller parameters for the *x*, *y*-position cotrol loops are determined by formulas as shown in (31).

$$\begin{aligned}k_{Px} &= 0.6k_{thx}; k_{Ix} = \frac{2k_{Px}}{\tau_{thx}}; k_{Dx} = \frac{k_{Px}\tau_{thx}}{8}\\ k_{Py} &= 0.6k_{thy}; k_{Iy} = \frac{2k_{Py}}{\tau_{thy}}; k_{Dy} = \frac{k_{Py}\tau_{thy}}{8}\end{aligned} \tag{31}$$

## 4. Modeling and Simulation of 6-DOF UAV Quadcopter Control System

### 4.1. Modeling 6-DOF UAV Quadcopter Control System

The study in this article utilizes the parameters of the UAV quadcopter as shown in Table 2.

**Table 2.** Parameters of the UAV quadcopter [8]

| Parameter | Symbol | Value |
|---|---|---|
| Quad. mass | $m$ | 0.468 $kg$ |
| Arm length | $l$ | 0.225 $m$ |
| Gravity | $g$ | 9.81$m/s^2$ |
| Inertia moment of the rotor | $I_M$ | 3.357e-5$kg.m^2$ |
| Thrust factor of rotor | $k$ | 2.980e-6$N.s^2$ |
| Drag coeffi. | $b$ | 1.140e-7 $N.m.s^2$ |
| Inertial constants | $I_{xx}$, $I_{yy}$ | 4.856e-3$kg.m^2$ |
| | $I_{zz}$ | 8.801e-3$kg.m^2$ |

The simulation diagram is obtained by modelling the dynamic model of the UAV quadcopter and building the PID control loops for UAV quadcopter on Matlab/Simulink, as shown in Fig. 5.

The dynamic model of the UAV quadcopter consits of three main blocks, which are:

- The block UAV quadrotor dynamic model block is built based on equations (1)-(22).
- The attitude and angulars positions control block calculate the thrust force and rotor torques for the UAV quadcopter, based on PID laws, using formulas (24)-(25).
- The translational position control block calculates the desired roll and pitch angles, based on PID laws, using formulas (29)-(31).

Applying this UAV quadcopter model, allows conducting experiments to determine PID parameters of quadcopter UAV control loops. This model also allows to evaluate the quality of the UAV control system with a defined PID controller.

### 4.2. The Experimental Parameter Determination of PID Controllers for UAV Quadcopter

Experiment to determine the parameters of six PID controllers for the UAV quadcopter using the Ziegler-Nichols method, in section 3. The control loops includes the $\psi$-yaw angle control loop, $\theta$-pitch angle control loop, $\phi$-roll angle control loop, *z*-attitude control loop, and *x*, *y*-position control loops.

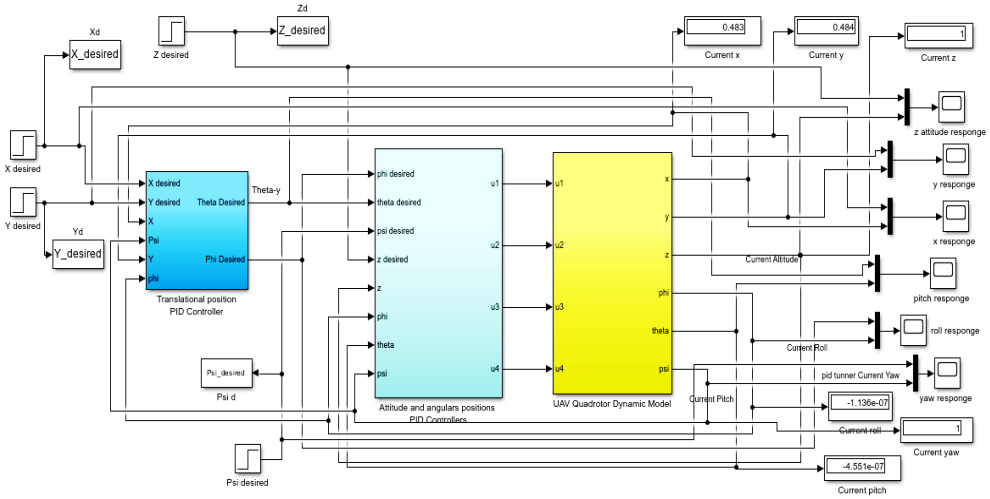


**Fig. 5.** Modelling the 6-DOF UAV quadcopter control system using PID controllers

Fig. 6 presents the experimental results for the $\psi$-yaw angle control loop. We obtain the $\psi$-yaw angle response with cycle oscillations at the value $k_{th} = 1.34$and oscillation period $t_{th} = 5.5s$.

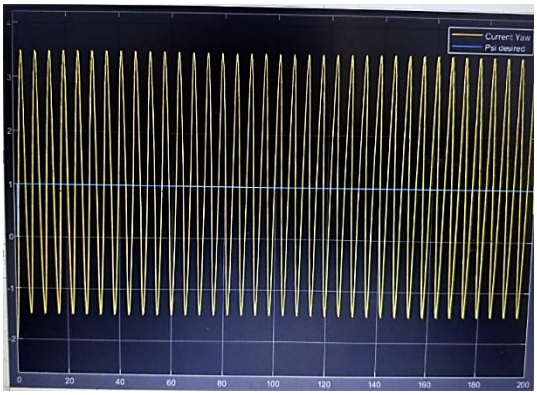


(a) Cycle oscillation, $k_{th}$=1.34

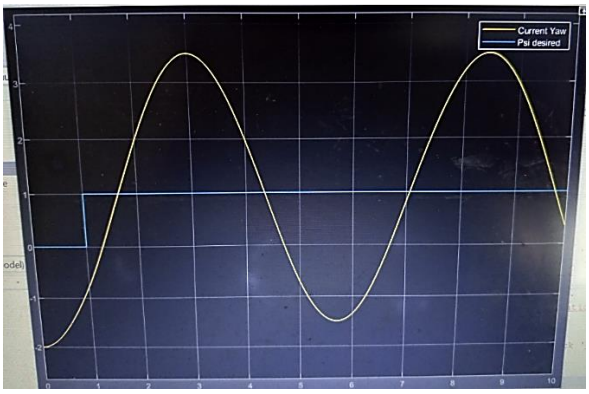


(b) Oscilation time cycle $t_{th} = 5.5s$

**Fig. 6.** Cycle oscillation response of $\psi$-yaw angle control loop

Therefore, according to the Ziegler-Nichols method, from the formula (25), we determine the PID controller parameters for the $\psi$-yaw angle control loop, as below.

$$k_{P\psi} = 0.804, k_{I\psi} = 0.29236, k_{D\psi} = 0.55275$$

Conducting similar experiments with the other control loops, we obtained the parameters of the PID controllers for the 6-DOF UAV quadcopter, as in Table 3.

**Table 3.** Parameters of PID controllers for 6-DOF UAV quadcopter

| Parameter of PID controllers | Position (x, y) | Altitude (z) | Roll ($\phi$) | Pitch ($\theta$) | Yaw ($\psi$) |
|---|---|---|---|---|---|
| $k_P$ | 0.00414 | 75 | 2.1 | 2.4 | 0.804 |
| $k_I$ | 0.0000345 | 42.8571 | 0.84 | 0.48 | 0.29236 |
| $k_D$ | 0.1242 | 32.8125 | 1.3125 | 3.09 | 0.55275 |

### 4.3. The PID Control System Simulation Results for UAV Quadcopter

Conducting simulation of the 6-DOF UAV quadcopter control system with the above proposed PID controllers and the desired values $\phi_d$= 0, $\theta_d$= 0, $\psi_d$=0.8rad/s, $x_d$=1m, $y_d$=1m, $z_d$=1m, we obtain the system responses as shown in Fig. 7, Fig. 8, Fig. 9, Fig. 10, Fig. 11, Fig. 12, Fig. 13.

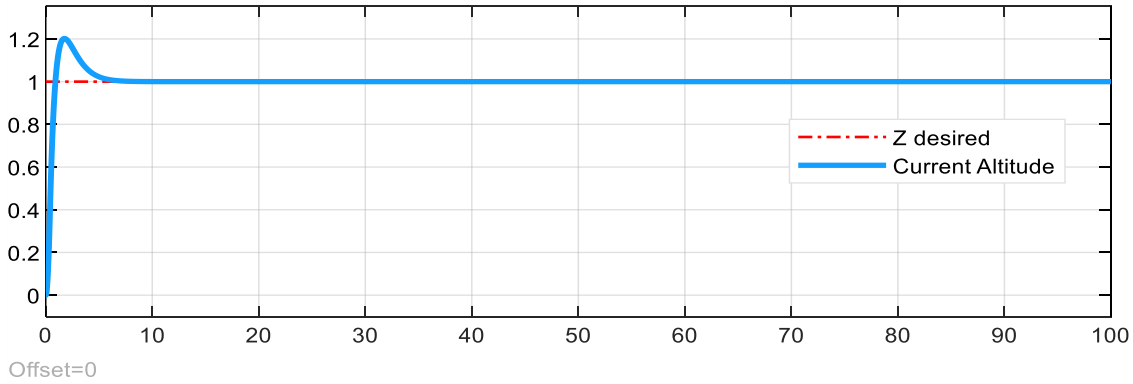


**Fig. 7.** The *z*-altitude response of the UAV quadcopter

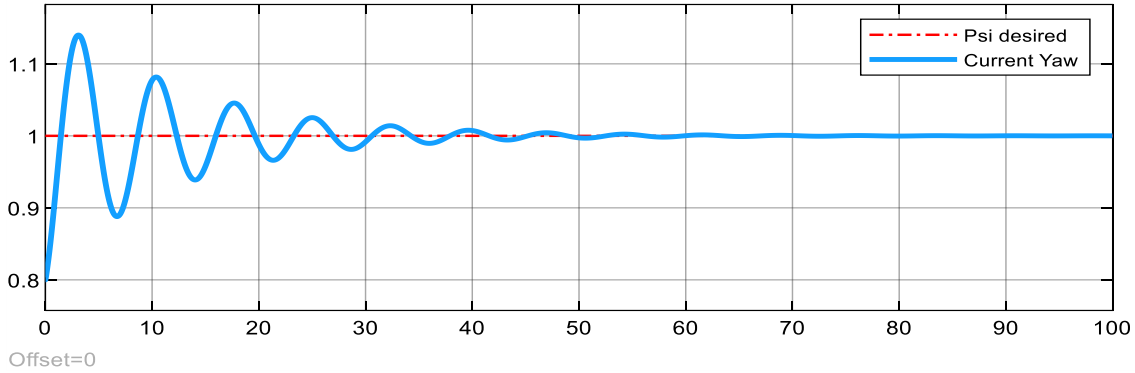


**Fig. 8.** The $\psi$-yaw response of the UAV quadcopter

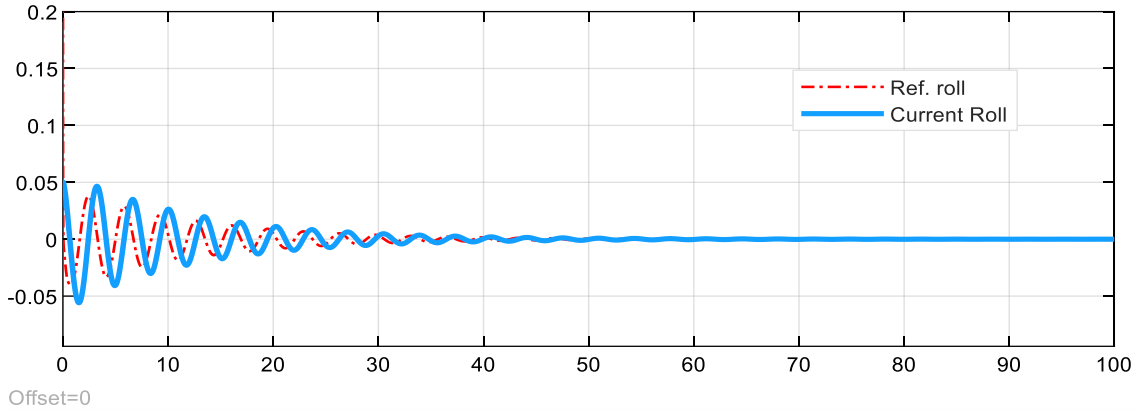


**Fig. 9.** The $\phi$-roll response of the UAV quadcopter

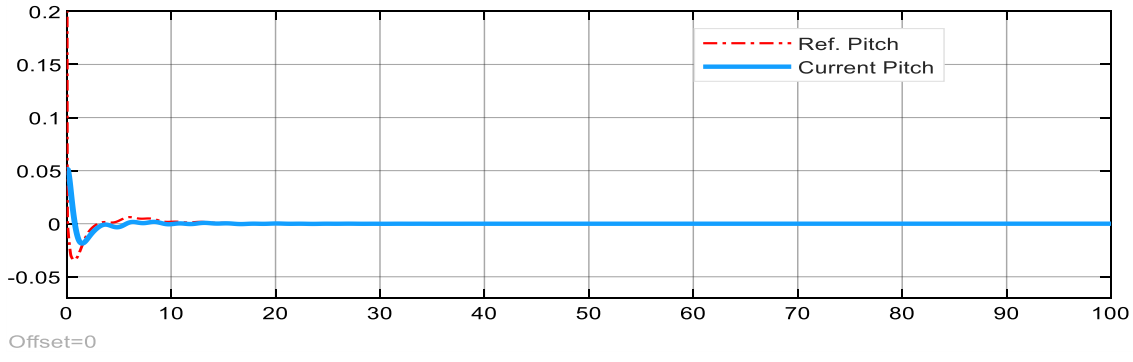


**Fig. 10.** The $\theta$-pitch response of the UAV quadcopter

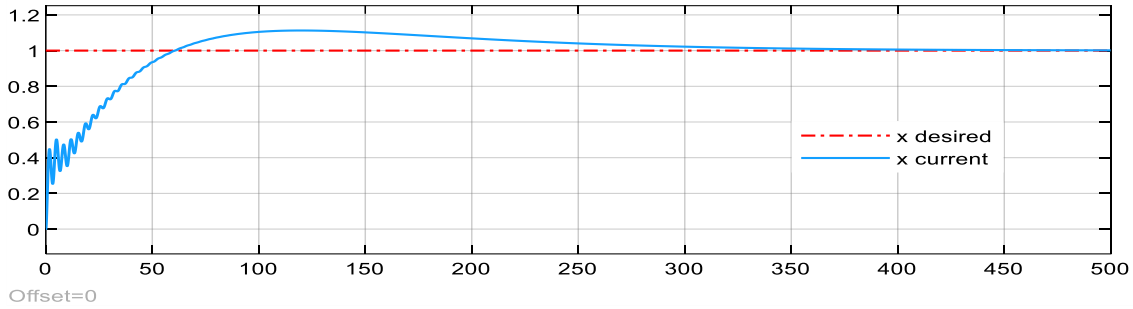


**Fig. 11.** The *x*-position response of UAV quadcopter

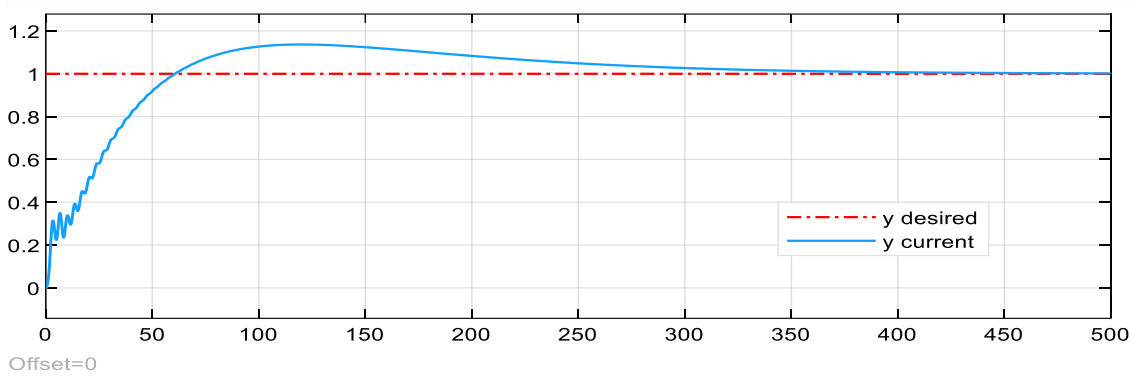


**Fig. 12.** The *y*-position response of UAV quadcopter

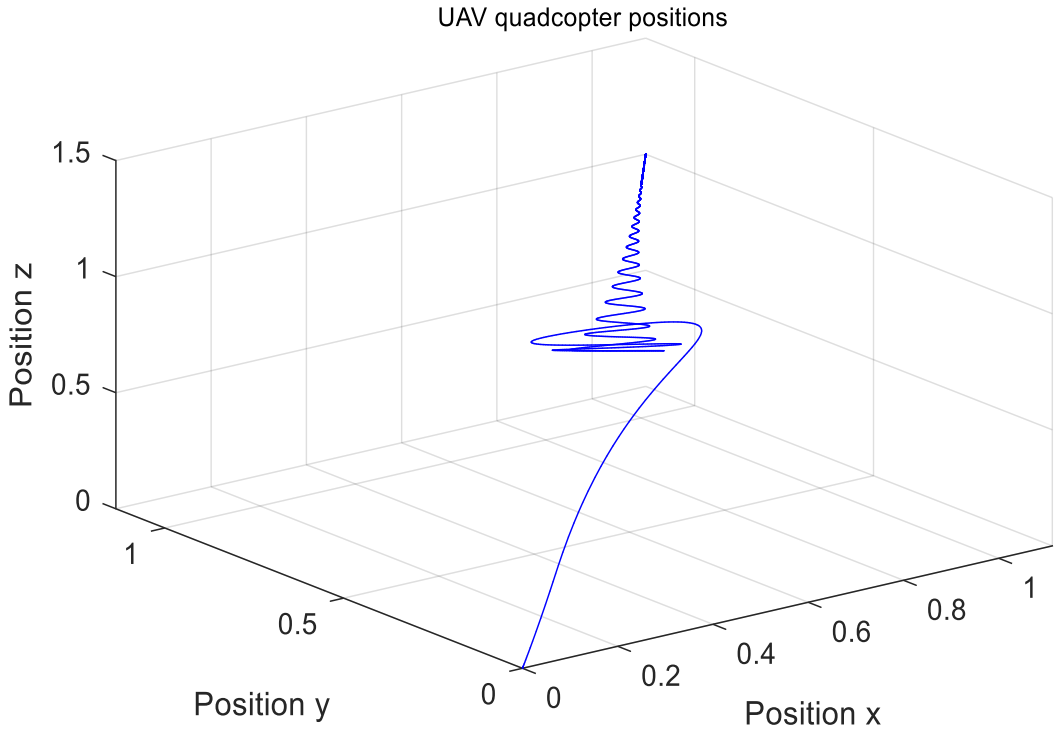


**Fig. 13.** The movement of UAV quadcopter in 3D x, y, z-axes

The output responses of the UAV quadcopter control system with the proposed PID controllers are depicted in Fig. 7, Fig. 8, Fig. 9, Fig. 10, Fig. 11, Fig. 12. The response of the *z*-altitude control loop is fastest, in which: steady-state error is zero, overshoot is 19.9%, rise time is 0.95s, steady time is 4.5s (Fig. 7). The response of the $\psi$-yaw angle control loop is initially fluctuating, specifically as follows: steady-state error is zero, overshoot is 15%, rise time is 1.45s, steady time is 49.5s (Fig. 8). The response

of the $\phi$-roll angle control loop is also initially fluctuating, specifically as follows: steady-state error is zero, overshoot is 4.5%, rise time is 0.55s, steady time is 39.5s (Fig. 9). The response of the $\theta$-pitch angle control loop is also fast, specifically as follows: steady-state error is zero, overshoot is 2.1%, rise time is 0.55 s, steady time is 9.8s (Fig. 10).

The responses of the *x, y*-position control loops is normal, specifically as follows: steady-state error is less than 1%, overshoot is 14.2%, rise time is 49.5s, steady time is 349.5s (Fig. 11, Fig. 12). The simulation results show that the responses of the *z*-altitude, $\psi$-angle, $\phi$-angle, $\theta$-angle control loops and *x, y*-position control loops for the UAV quadcopter ensured the flight balance stablility at the desired positions with overshoot less than 20%, steady-state error approximate 0, rise time from 1s to less than 50s. The quality indexes of the UAV quadcopter control system using the above proposed PID controllers are determined and shown clearly in Table 4.

**Table 4.** The quality indexes of the UAV quadcopter control system

| Controller / Quality index | PID *z*-altitude | PID $\psi$-angle | PID $\phi$-angle | PID $\theta$-angle | PID *x, y*-positions |
|---|---|---|---|---|---|
| Rise time | Small, <1s | Small, <1.5s | Small, <1s | Small, <1s | Large, <50s |
| Steady time | Small, <5s | Normal, <50s | Normal, <40s | Small, <10s | Large, <350s |
| Overshoot | Normal, <20% | Normal, <15% | Small, <5% | Small, <5% | Normal, <15% |
| Steady-state error | Zero, 0 | Zero, 0 | Zero, 0 | Zero, 0 | Less, <1% |

The control system quickly brings the UAV quadcopter to the desired *z*-altitude position and $\psi$-angle, $\phi$-angle, $\theta$-angle, and then UAVquadcopter is controlled stability at the *x,y*-positions. The positons responses in the space of the UAV quadcopter are desmotrated in 3D *x,y,z*-coordinate system, as shown in Fig. 13. From the Fig. 13, it can be seen that the UAV quadcopter flight trajectory quickly reaches the desired position, however there are fluctuations in roll and yaw angles when the UAV departs. This decreases rapidly upon reaching the desired destination position.

## 5. Conclusion

The article has researched and developed in detail two rotational and translational dynamic models of the 6-DOF UAV quadcopter - this is a strong-nonlinear and complex control object. And then, analyzing its dynamic model, the article introduces the the two-loop cascade control structure for 6-DOF UAV quadcopter: the inner control loops have four feedback control loops of three Euler angles and *z*-altitude; the outer control loop have two feedback control loops of the *x, y*-positions. And then, based on the UAV each part dynamic model, the article presents proposed the simple method and formulas to determine PID controller parameters for these 6 control loops, which are $\psi$-yaw angle control loop, $\theta$-pitch angle control loop, $\phi$-roll angle control loop, *z*-attitude control loop, and *x, y*-positions control loops, on the basis of applying the Ziegler-Nichols experimental method. Finally, the simulation model of UAV quadcopter is developed in Matlab/Simulink. Then, perform simulation to evaluate the UAV quadcopter control system quality with above proposed PID controllers.

The simulation results show that the proposed PID controllers have controlled and stabilized the flight balance for UAV quadcopter at the desired positions with overshoot less than 20%, steady-state error **a**pproximate 0. The research results show the prospect of applying the poposed PID controllers in practical control of UAVs transporting goods, due to its simplicity and ease of implementation on microcontroller circuit board, as well as convenient PID parameters adjustment method.

However, this UAV quadcopter two-loop cascade control system only responds well to small disturbances. For large disturbances, the heuristic method for the PID parameters adjustments is recommended.

Therefore, to reduce the impact of disturbances on UAVs, future research, in addition to continuing to conduct the proposed PIDs algorithms on physical UAVs, the authors will develop self-tuning intelligent PID control algorithms, intelligent control algorithms and nonlinear control,

applying in fuzzy logic, neural networks, model predictive control ensuring the position control and flight stability cotrol, trajectory tracking control for UAV quadcopter.

**Author Contribution:** All authors contributed equally to the main contributor to this paper. All authors read and approved the final paper.

**Acknowledgements:** This research is funded by University of Transport and Communications (UTC) under grant number T2024-DT-005.

**Conflicts of Interest**: The authors declare no conflicts of interest.

## References

[1] G. Hoffmann, H. Huang, S. Waslander, and C. Tomlin, "Quadrotor helicopter flight dynamics and control: Theory and experiment," *Proceedings of the AIAA Guidance, Navigation and Control Conference and* Exhibit, pp. 1-20, 2007, https://doi.org/10.2514/6.2007-6461.

[2] H. Huang, G. M. Hoffmann, S. L. Waslander and C. J. Tomlin, "Aerodynamics and control of autonomous quadrotor helicopters in aggressive maneuvering," *2009 IEEE International Conference on Robotics and Automation*, pp. 3277-3282, 2009, https://doi.org/10.1109/ROBOT.2009.5152561.

[3] A. A. Mian, W. Daobo, "Modeling and backstepping-based nonlinear control strategy for a 6 DOF quadrotor helicopter," *Chinese Journal of Aeronautics*, vol. 21, no. 3, pp. 261-268, 2008, https://doi.org/10.1016/S1000-9361(08)60034-5.

[4] C. Ha, Z. Zuo, F. B. Choi, and D. Lee, "Passivity-based adaptive backstepping control of quadrotor-type UAVs," *Robotics and Autonomous Systems*, vol. 62, no. 9, pp. 1305-1315, 2014, https://doi.org/10.1016/j.robot.2014.03.019.

[5] V. Nekoukar and N. M. Dehkordi, "Robust path tracking of a quadrotor using adaptive fuzzy terminal sliding mode control," *Control Engineering Practice*, vol. 110, p. 104763, 2021, https://doi.org/10.1016/j.conengprac.2021.104763.

[6] H. Housny, E. A. Chater and H. El Fadil, "New Deterministic Optimization Algorithm for Fuzzy Control Tuning Design of a Quadrotor," *2019 5th International Conference on Optimization and Applications (ICOA)*, pp. 1-6, 2019, https://doi.org/10.1109/ICOA.2019.8727622.

[7] Q. Jiao, J. Liu, Y. Zhang and W. Lian, "Analysis and design the controller for quadrotors based on PID control method," *2018 33rd Youth Academic Annual Conference of Chinese Association of Automation (YAC)*, pp. 88-92, 2018, https://doi.org/10.1109/YAC.2018.8406352.

[8] D. S. Vamsi, T. V. S. Tanoj, U. M. Krishna and M. Nithya, "Performance Analysis of PID controller for Path Planning of a Quadcopter," *2019 2nd International Conference on Power and Embedded Drive Control (ICPEDC)*, pp. 116-121, 2019, https://doi.org/10.1109/ICPEDC47771.2019.9036558.

[9] A. S. Elkhatem and S. N. Engin, "Robust LQR and LQR-PI control strategies based on adaptive weighting matrix selection for a UAV position and attitude tracking control," *Alexandria Engineering Journal*, vol. 61, no. 8, pp. 6275-6292, 2022, https://doi.org/10.1016/j.aej.2021.11.057.

[10] C. E. Luis, M. Vukosavljev and A. P. Schoellig, "Online Trajectory Generation With Distributed Model Predictive Control for Multi-Robot Motion Planning," *IEEE Robotics and Automation Letters*, vol. 5, no. 2, pp. 604-611, 2020, https://doi.org/10.1109/LRA.2020.2964159.

[11] C. -C. Chen and Y. -T. Chen, "Feedback Linearized Optimal Control Design for Quadrotor With Multi-Performances," *IEEE Access*, vol. 9, pp. 26674-26695, 2021, https://doi.org/10.1109/ACCESS.2021.3057378.

[12] M. Labbadi, Y. Boukal, M. Cherkaoui, and M. Djemai, "Fractional-order global sliding mode controller for an uncertain quadrotor UAVs subjected to external disturbances," *Journal of the Franklin Institute*, vol. 358, no. 9, pp. 4822-4847, 2021, https://doi.org/10.1016/j.jfranklin.2021.04.032.

[13] Teppo Luukkonen, "Modelling and control of quadcopter," *School of Science*, pp. 1-24, 2011, https://sal.aalto.fi/publications/pdf-files/eluu11_public.pdf.

[14] S. Yang and B. Xian, "Exponential Regulation Control of a Quadrotor Unmanned Aerial Vehicle With a Suspended Payload," *IEEE Transactions on Control Systems Technology*, vol. 28, no. 6, pp. 2762-2769, 2020, https://doi.org/10.1109/TCST.2019.2952826.

[15] T. Bresciani, "Modelling Identification and Control of a Quadrotor Helicopter," *MSc theses*, 2008, https://lup.lub.lu.se/luur/download?func=downloadFile&recordOId=8847641&fileOId=8859343.

[16] A. N. Muhsen, S. M. Raafat, "Optimized PID Control of Quadrotor System Using Extremum Seeking Algorithm," *Engineering and Technology Journal*, vol. 39, no. 6, pp. 996-1010, 2021, https://doi.org/10.30684/etj.v39i6.1850.

[17] G. Bachelor, E. Brusa, D. Ferretto and A. Mitschke, "Model-Based Design of Complex Aeronautical Systems Through Digital Twin and Thread Concepts," *IEEE Systems Journal*, vol. 14, no. 2, pp. 1568-1579, 2020, https://doi.org/10.1109/JSYST.2019.2925627.

[18] S. Zhao, K. Lu, S. Wu and D. Su, "Helicopter Flight Dynamics Modeling Using Simulink," *2021 33rd Chinese Control and Decision Conference (CCDC)*, pp. 2591-2596, 2021, https://doi.org/10.1109/CCDC52312.2021.9601647.

[19] S. Abdelhaya, A. Zakriti, "Modeling of a Quadcopter Trajectory Tracking System Using PID controller," *Procedia Manufacturing*, vol. 32, pp. 564–571, 2019, https://doi.org/10.1016/j.promfg.2019.02.253.

[20] X. Zhou *et al*., "Safety Flight Control Design of a Quadrotor UAV With Capability Analysis," *IEEE Transactions on Cybernetics*, vol. 53, no. 3, pp. 1738-1751, 2023, https://doi.org/10.1109/TCYB.2021.3113168.

[21] P. Castillo, R. Lozano and A. Dzul, "Stabilization of a mini rotorcraft with four rotors," *IEEE Control Systems Magazine*, vol. 25, no. 6, pp. 45-55, 2005, https://doi.org/10.1109/MCS.2005.1550152.

[22] G. V. Raffo, M. G. Ortega, F. R. Rubio, "An integral predictive/nonlinear H∞ control structure for a quadrotor helicopter," *Automatica*, vol. 46, no. 1, pp. 29-39, 2010, https://doi.org/10.1016/j.automatica.2009.10.018.

[23] K. J. Astrom and T. Hagglund, "Advanced PID Control," *Instrumentation, Systems and Automation Society*, 2006, https://portal.research.lu.se/en/publications/advanced-pid-control.

[24] A. T. Bayisa, "Controlling Quadcopter Altitude using PID-Control System," *International Journal of Engineering Research & Technology*, vol. 08, no. 12, pp. 195-199, 2019, https://doi.org/10.17577/IJERTV8IS120118.

[25] N. H. Sahrir, M. A. M. Basri, "Modelling and Manual Tuning PID Control of Quadcopter," *Control, Instrumentation and Mechatronics: Theory and Practice*, pp. 346-357, 2022, https://doi.org/10.1007/978-981-19-3923-5_30.

[26] D. Kotarski, Z. Benić, M. Krznar, "Control Design for Unmanned Aerial Vehicles with Four Rotors," *Interdisciplinary Description of Complex Systems*, vol. 14, no. 2, pp. 236-245, 2016, http://dx.doi.org/10.7906/indecs.14.2.12.

[27] I. C. Dikmen, A. Arisoy and H. Temeltas, "Attitude control of a quadrotor," *2009 4th International Conference on Recent Advances in Space Technologies*, pp. 722-727, 2009, https://doi.org/10.1109/RAST.2009.5158286.

[28] M. L Luyben and W. L Luyben, "Essentials of Process Control," *McGraw*-Hill, 1997, https://books.google.co.id/books/about/Essentials_of_Process_Control.html?id=ONBTAAAAMAAJ&redir_esc=y.

[29] E. N. Mobarez, A. Sarhan and M. Ashry, "Fractional order PID Based on a Single Artificial Neural Network Algorithm for Fixed wing UAVs," *2019 15th International Computer Engineering Conference (ICENCO)*, pp. 1-7, 2019, https://doi.org/10.1109/ICENCO48310.2019.9027378.

[30] D. Nouman, T. Hussain, "Development of PID Controller Tuned by using Ziegler Nichols Method for Controlling the Fluid Level in Coupled Tank System," *3rd International Conference on Innovative Academic Studies*, vol. 3, no. 1, pp. 646-670, 2023, https://doi.org/10.59287/icias.1606.

[31] C. V. Nguyen and M. T. Nguyen, "Design and Simulation of PID-Based Control System for UAV Quadcopters," *Advances in Information and Communication Technology*, pp. 146-153, 2024, https://doi.org/10.1007/978-3-031-50818-9_18.

[32] A. Abdulkareem, V. Oguntosin, O. M. Popoola and A. A. Idowu, "Modeling and Nonlinear Control of a Quadcopter for Stabilization and Trajectory Tracking," *Journal of Engineering*, vol. 2022, 2022, https://doi.org/10.1155/2022/2449901.

[33] N. H. Abbas, A. R. Sam, "Tuning of PID Controllers for Quadcopter System using Hybrid Memory based Gravitational Search Algorithm – Particle Swarm Optimization," *International Journal of Computer Applications*, vol. 172, no. 4, pp. 9-18, 2017, https://doi.org/10.5120/ijca2017915125.

[34] A. Baharuddin and M. A. M. Basri, "Trajectory Tracking of a Quadcopter UAV using PID Controller," *ELEKTRIKA Journal of Electrical Engineering*, vol. 22, no. 2, pp. 14-21, 2023, https://doi.org/10.11113/elektrika.v22n2.440.

[35] A. Noordin, M. A. M. Basri, Z. Mohamed, "Simulation and experimental study on PID control of a quadrotor MAV with perturbation," *Bulletin of Electrical Engineering and Informatics*, vol. 9, no. 5, pp. 1811-1818, 2020, https://doi.org/10.11591/eei.v9i5.2158.

[36] A. M. A, Abdul Saleem, "Quadrotor Modelling Approaches and Trajectory Tracking Control algorithms: A Review," *International Journal of Robotics and Control Systems*, vol. 4, no. 1, pp. 401-426, 2024, https://doi.org/10.31763/ijrcs.v4i1.1324.

[37] M. Maaruf, M. S. Mahmouda, A. Ma'arif, "A Survey of Control Methods for Quadrotor UAV," *International Journal of Robotics and Control Systems*, vol. 2, no. 4, pp. 652-665, 2022, https://doi.org/10.31763/ijrcs.v2i4.743.

[38] M. Karahan, M. Inala, C. Kasnakoglu, "Fault Tolerant Super Twisting Sliding Mode Control of a Quadrotor UAV Using Control Allocation," *International Journal of Robotics and Control Systems*, vol. 3, no. 2, pp. 270-285, 2023, https://doi.org/10.31763/ijrcs.v3i2.994.

[39] A. Daadi, H. Boulebtinaia, S. H. Derrouaouia, F. Boudjema, "Sliding Mode Controller Based on the Sliding Mode Observer for a QBall 2+ Quadcopter withExperimental Validation," *International Journal of Robotics and Control Systems*, vol. 2, no. 2, pp. 332-356, 2022, https://doi.org/10.31763/ijrcs.v2i2.693.

[40] N. H. Sahrir, A. M. Basri, "Radial Basis Function Network Based Self-Adaptive PID Controller for Quadcopter," *International Journal of Robotics and Control Systems*, vol. 4, no. 1, pp. 151-173, 2024, https://doi.org/10.31763/ijrcs.v4i1.1261.

[41] Z. Qi, "On the use of PID control to improve the stability of the quad-rotor UAV," *Proceedings of the 4th International Conference on Signal Processing and Machine Learning*, vol. 49, pp. 31-36, 2024, https://doi.org/10.54254/2755-2721/49/20241054.

[42] H. Zhao, "Classical PID Control of a Quadcopter UAV Under Variable Load Conditions," *Academic Journal of Science and Technology*, vol. 9, no. 2, pp. 44-46, 2024, https://doi.org/10.54097/13m5xg10.

[43] M. F. Pairan, S. Shamsudin, M. F. Yaakub, "Autotuning PID Controllers for Quadplane Hybrid UAV using Differential Evolution Algorithm," *Journal of Aeronautics, Astronautics and Aviation*, vol. 56, no. 1s, pp. 341-356, 2024, https://doi.org/10.6125/JoAAA.202403_56(1S).23.

[44] T. A. Lohani, A. Dixit, P. Agrawal, "Adaptive PID Control for Autopilot Design of Small Fixed Wing UAVs," *MATEC Web of Conferences*, vol. 393, p. 03005, 2024, https://doi.org/10.1051/matecconf/202439303005.

[45] D. Wan, M. Zhao, W. Mo, L. Peng, J. Wang, G. Liang, "Research on Control Method of Four Rotor UAV Based on Classical PID Control System," *Smart Grid and Innovative Frontiers in Telecommunications*, pp. 502-512, 2023, https://doi.org/10.1007/978-3-031-31733-0_43.

[46] D. Lv, C. Liang, Y. Zhang, "Research and Design of Four Rotor UAV Based on Cascade PID," *Advances in Artificial Systems for Medicine and Education VI*, pp. 88-99, 2023, https://doi.org/10.1007/978-3-031-24468-1_9.

[47] L. Zhou, A. Pljonkin, P. K. Singh, "Modeling and PID control of quadrotor UAV based on machine learning," *Journal of Intelligent Systems*, vol. 31, no. 1, pp. 1112-1122, 2022, https://doi.org/10.1515/jisys-2021-0213.

[48] K. Chen, "Controller design for transition flight of rotor-driven VTOL fixed-wing UAV based on PID," *Proceedings of the 2023 International Conference on Mechatronics and Smart Systems*, vol. 9, pp. 15-21, 2023, https://doi.org/10.54254/2755-2721/9/20230018.

[49] A. Ma'arif, I. Suwarno, E. Nur'aini, N. M. Raharja, "Altitude Control of UAV Quadrotor Using PID and Integral State Feedback," *BIO Web of Conferences*, vol. 65, p. 07011, 2023, https://doi.org/10.1051/bioconf/20236507011.

[50] H. Song, S. Hu, W. Jiang, Q. Guo, "EKF-AF PID-Based Attitude Control Algorithm for UAVs," *Mobile Information Systems*, vol. 2022, 2022, https://doi.org/10.1155/2022/1543949.

[51] G. Sheng and G. Gao, "Research on the Attitude Control of Civil Quad-Rotor UAV Based on Fuzzy PID Control," *2019 Chinese Control And Decision Conference (CCDC)*, pp. 4566-4569, 2019, https://doi.org/10.1109/CCDC.2019.8832855.

[52] M. Jiang, "Application of Fuzzy PID Control in UAV Control System," *2021 Third International Conference on Inventive Research in Computing Applications (ICIRCA)*, pp. 197-200, 2021, https://doi.org/10.1109/ICIRCA51532.2021.9544986.